# Supporting Information

# Different Photostability of $BiVO_4$ in Near-pH-Neutral Electrolytes

Siyuan Zhang,* Ibbi Ahmet, Se-Ho Kim, Olga Kasian, Andrea M. Mingers, Patrick Schnell, Moritz Kölbach, Joohyun Lim, Anna Fischer, Karl J. J. Mayrhofer, Serhiy Cherevko, Baptiste Gault, Roel van de Krol,* and Christina Scheu*

## Experimental Details

**Photoanode Preparation:**

$BiVO_4$ was deposited on fluorine-doped tin oxide (FTO) coated glass (TEC7, Pilkington) by pulsed laser deposition (PLD) in vacuum ($<2\times10^{-6}$ mbar) at room temperature. The laser fluence, spot size and pulse frequency were set to 1.5 J $cm^{-2}$, 1.3×2 $mm^2$ and 10 Hz, respectively. The target-to-substrate distance was 60 mm. Further details on the PLD system and the $BiVO_4$ target are reported elsewhere.[24] After deposition, the films were annealed at 450 °C in air for 2 h.

**Illuminated SFC-ICPMS Setup:**

As detailed in a previous report,[23] photoelectrochemical (PEC) experiments were performed through a scanning flow cell (SFC) controlled by a Reference600 potentiostat (Gamry). The SFC was positioned to contact the $BiVO_4$ working electrode and limits the area to 1 $mm^2$. A Pt-wire (0.5 mm, 99.997%, Alfa Aesar) counter electrode and a saturated Ag/AgCl reference electrode (Metrohm) were respectively placed in the inlet and outlet channels of the SFC. The borate buffer (pH=9.3–9.4) was prepared from $Na_2B_4O_7$ (15 mM, Merck, suprapure). The phosphate buffer (pH=7.1–7.2) was prepared from $KH_2PO_4$ (5.2 mM, Merck, suprapure) and $Na_2HPO_4$ (8.2 mM, Merck, suprapure). The citrate buffer (pH=6.9–7) was prepared from $C_6H_8O_7{\cdot}H_2O$ (15 mM, Merck, p.A.) and NaOH (44.1 mM, Merck, Titrisol). To ensure accurate evaluation of $V_{RHE}$, electrolytes were measured by a MultiLab540 pH-meter (WTW) on a daily basis.

Electrolytes were pumped through the SFC at 3.4 µL $s^{-1}$ and analyzed online in a NexION300X inductively coupled plasma mass spectrometer (ICPMS) (Perkin Elmer). For time-resolved analysis of the amount of dissolved ions, the detected intensities of $^{51}V$ and $^{209}Bi$ isotopes were analyzed with respect to an internal standard for compensation of physical interferences: $^{89}Y$ was used for V, and $^{187}Re$ for Bi. Both elements were added to the electrolyte via a Y-shaped connector in a solution of 0.5% $HNO_3$ (65%, Merck, suprapure) behind the SFC. ICPMS calibration was performed on a daily basis prior to the measurements and used to convert the detected intensities to the concentration of the dissolved ions in the electrolyte. A Superlite S04 light (Lumatec) filtered to 400–700 nm was guided to illuminate the front side of $BiVO_4$, with intensity calibrated to 100 mW $cm^{-2}$ using a Si-diode photometer (Newport).

**Structural Characterization:**

X-ray photoelectron spectroscopy (XPS) was measured on a Quantera II (Physical Electronics) using a monochromatic Al-Kα X-ray source (1486.6 eV) operated at 15 kV and 25 W, and analyzed by the Casa XPS software.

Scanning electron microscopy (SEM) micrographs were taken using a Scios microscope (Thermo Fisher) operated at 10 kV using a secondary electron detector.

For cross-sectional view by scanning transmission electron microscopy (STEM), thin foils were prepared using focused ion beam (FIB) milling. STEM was performed on a Titan Themis microscope (Thermo Fisher) operated at 300 kV, with an aberration-corrected electron probe of 23.8 mrad convergence and a lateral resolution of 0.1 nm. Annular dark field (ADF) and annular bright field (ABF) micrographs were formed using electrons scattered to 73−200 and 8−16 mrad, respectively.

Needle-shaped samples for atom probe tomography (APT) were prepared using FIB milling, following the procedures reported by Thompson *et al.* (Thompson, K.; Lawrence, D.; Larson, D. J.; Olson, J. D.; Kelly, T. F.; Gorman, B. In Situ Site-Specific Specimen Preparation for Atom Probe Tomography. *Ultramicroscopy* **2007,** *107*, 131). APT measurements were conducted on a LEAP5000XS (CAMECA) at 70 K base temperature, in pulsed laser mode at 2% detection rate, 60 pJ pulse energy, and 125 kHz pulse frequency. 3D reconstruction and composition were analyzed using IVAS 3.8.4 software.

## Controlled Electrochemical Experiments in the Dark

Photocorrosion usually refers to degradation of the electrode caused by photoelectrochemical (PEC) processes triggered by the transfer of photo-generated minority carriers, but it may well be compounded by electrochemical (EC) processes that only involve transfer of majority carriers and chemical processes that do not involve any charge transfer.

The same cyclic voltammetry (CV) scans as shown in Figure 1 were conducted in the dark and plotted individually in Figure S1. As in Figure 1, a contact current is observed, *i.e.*, a current that flows after the electrolyte in the scanning flow cell (SFC) is connected to the working electrode. During subsequent scans between 0.4 and 1.6 $V_{RHE}$, the dark current is negligible.

As shown by the dissolution rates in Figure S1, Bi dissolution was not observed in the dark. The first dissolution peak of V was observed as the working electrode established contact with the electrolyte from SFC, and hence named "**contact dissolution**". During the first potential scan from 0.4 to 1.6 $V_{RHE}$, a V dissolution peak was observed in the borate and phosphate, and termed "**EC dissolution**". Both transient dissolution peaks are also observed during the experiments under illumination. For example, as shown in Figure 1, a higher amount of V dissolution was observed during the first potential scan from 0.4 to 1.6 $V_{RHE}$ than the subsequent cycles under illumination, which is interpreted as the superposition of EC and **PEC dissolution**.

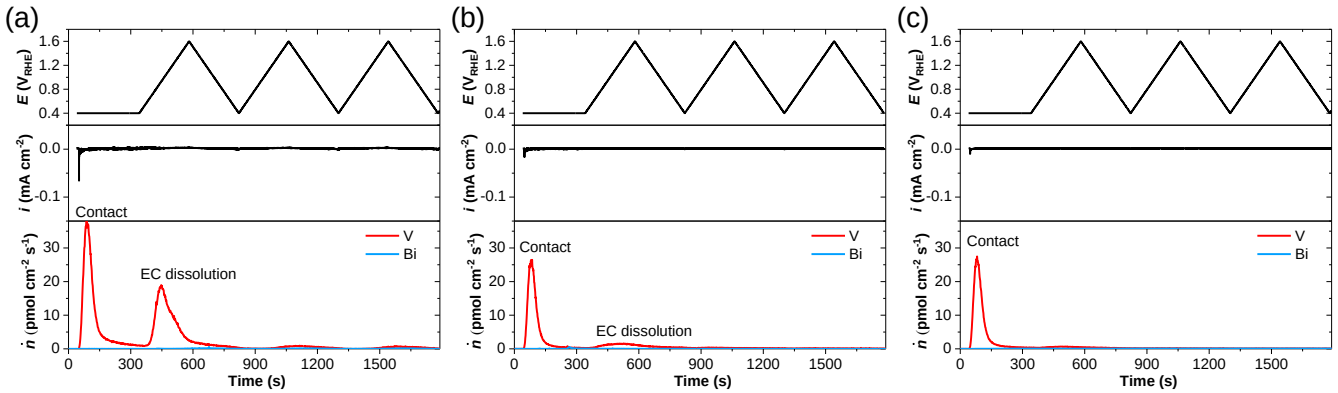


**Figure S1.** Time profiles of applied potential to the $BiVO_4$ photoanode, current density *i*, Bi and V dissolution rates *ṅ* in the dark in (a) borate, (b) phosphate, and (c) citrate electrolytes.

## Analysis of Dissolution Peaks

As shown in Figure S2, the replot of data in Figure 1 with respect to the applied potential helps tracking the repeating PEC dissolution features during the CV cycles. As EC dissolution peaks appear during the first CV scan (first row of Figure S2), we rely on the second and third CV scans (second and third rows of Figure S2) to analyze the PEC dissolution peaks.

In borate (left column of Figure S2), V and Bi dissolution is mostly synchronous. V and Bi dissolution peaks are very close in magnitude and position, at ~1.6 $V_{RHE}$ and ~1.2 $V_{RHE}$ in the anodic and cathodic scans, respectively.

In phosphate (middle column of Figure S2), V dissolution peaks at ~1.5 $V_{RHE}$ in the cathodic scan, whereas Bi dissolution shows two peaks, ~1.1 $V_{RHE}$ in the anodic scan and ~0.8 $V_{RHE}$ in the cathodic scan.

It is noteworthy that Bi dissolution peaks are correlated to the oxygen evolution reaction (OER). The photocurrent onset at ~0.8 $V_{RHE}$ overlaps with the onset of Bi dissolution in the anodic direction, which is more obvious in the first CV cycle (Figure S2a, S2b) where no preceding Bi dissolution happened.

In citrate (right column of Figure S2), V and Bi dissolution rates fluctuate much less with potential, staying around a constant rate of ~2 pmol $cm^{-2}$ $s^{-1}$.

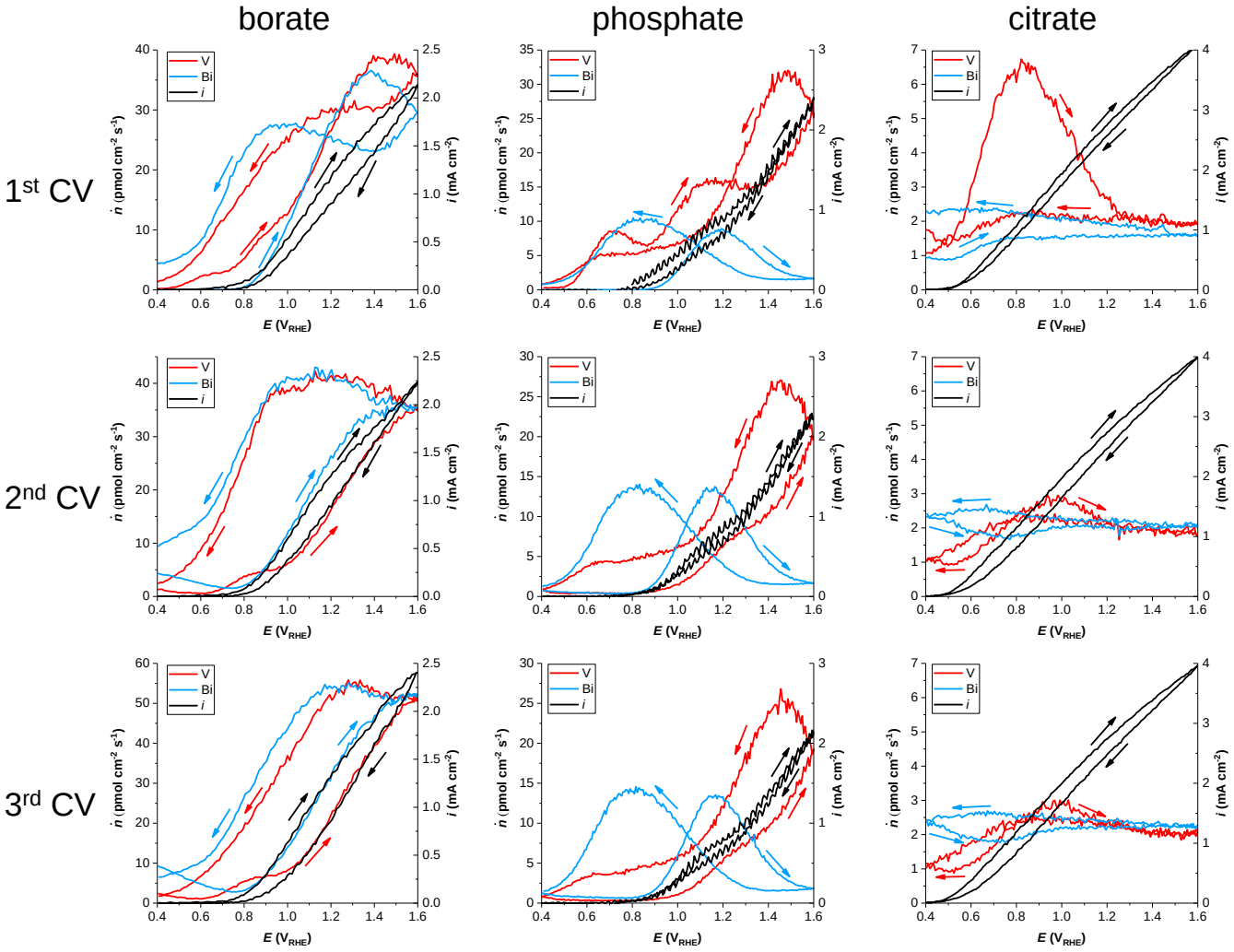


**Figure S2.** Dissolution rates ($\dot{n}$) and photocurrent density ($i$) plotted against potential ($E$) during the first, second, and third CV cycles (arranged in rows) from the datasets in Figure 1 under illumination in borate, phosphate, and citrate electrolytes (arranged in columns).

## Surface Composition and Morphology

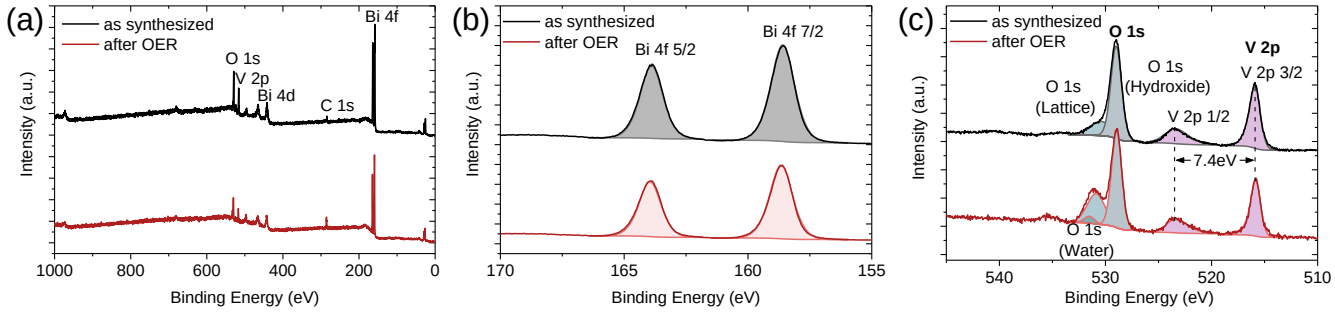


**Figure S3.** X-ray photoelectron spectroscopy (XPS) (a) survey, (b) Bi 4f, (c) V 2p and O 1s spectra measured from the $BiVO_4$ film regions outside of the SFC contact area (*i.e.*, as synthesized) and within the SFC contact area, after OER for ~20 min in borate.

**Table S1.** Surface composition determined from XPS spectra in Figure S3.

| | V molar fraction (at.%) | Bi molar fraction (at.%) |
|---|---|---|
| As-synthesized | 59.1 ± 1.1 * | 40.9 ± 1.1 |
| After OER | 50.6 ± 2.1 | 49.4 ± 2.1 |

* Each error bar shows statistical variance from 6 measurements on 3 spots.

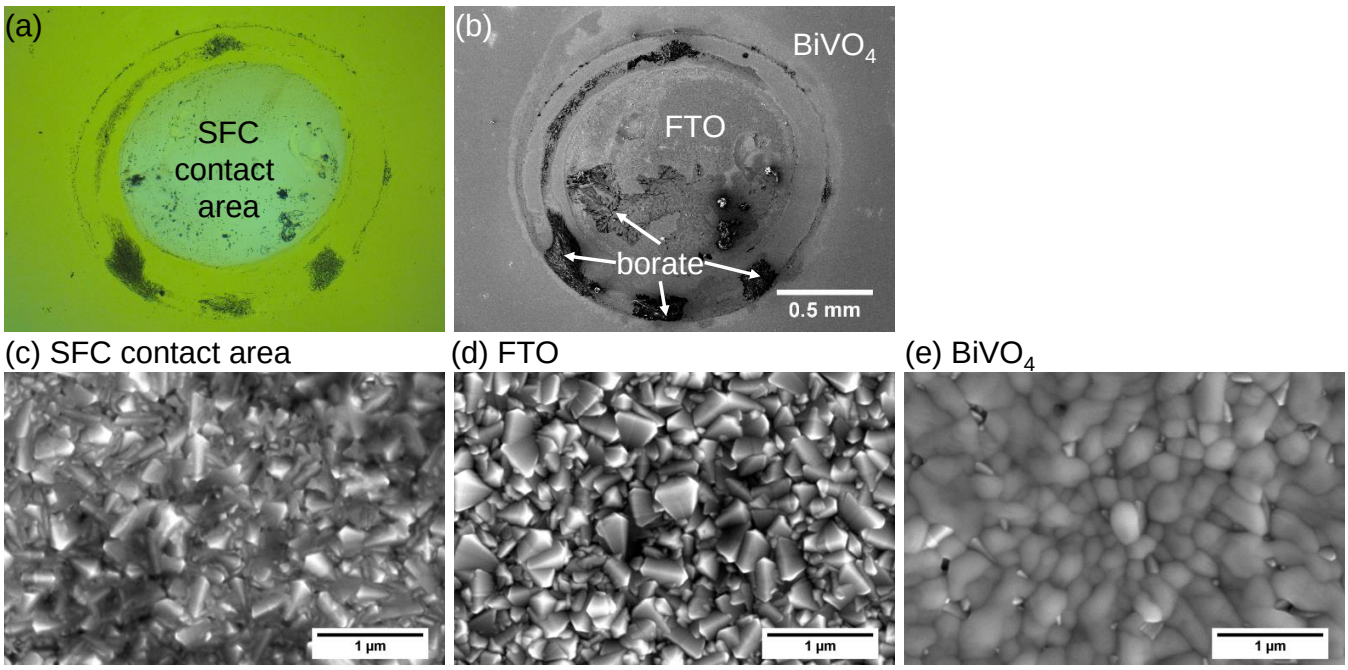


**Figure S4.** (a) Optical micrograph in transmittance and (b) scanning electron microscopy top-view micrograph of the SFC contact area after the chronoamperometric measurement in Figure 2. (c) Magnified view on the surface morphology within the SFC contact area in comparison with (d) bare FTO surface and (e) $BiVO_4$ surface outside the SFC contact area.

## Atom Probe Tomography (APT)

APT differentiates ions reaching the spectrometer at different time of flight and relates them to their respective mass-to-charge ratios. The major ions and compound ions detected from the $BiVO_4$ film and their spatial distribution are shown in Figure S5b. Quantification of atomic concentrations is feasible, as shown in a line profile across the $BiVO_4$/FTO interface in Figure S5d. There is deviation from the nominal $BiVO_4$ stoichiometry (Bi: 16.7 at.%, V: 16.7%, O: 66.7%), especially the underestimation of O content. This is a phenomenon observed in many oxide compounds, and attributed to the evaporation of neutral-charged atomic clusters such as $O^0$ and $O_2{}^0$, which could not be detected by the spectrometer (Gault, B.; Saxey, D. W.; Ashton, M. W.; Sinnott, S. B.; Chiaramonti, A. N.; Moody, M. P.; Schreiber, D. K. Behavior of Molecules and Molecular Ions Near a Field Emitter. *New J. Phys.* **2016,** *18*, 033031). Nevertheless, APT provides unmatched sensitivity and nanometer resolution to detect local deviation in composition.

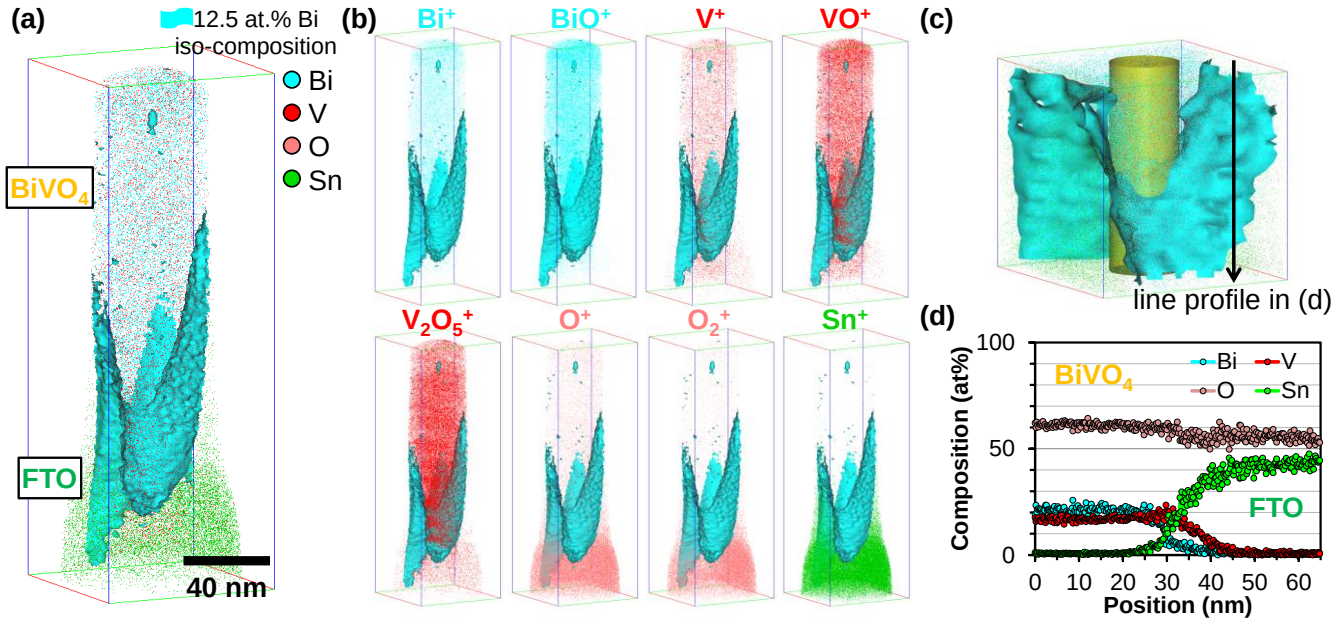


**Figure S5.** (a) 3D atom map evaluated from (b) 3D ion maps of $BiVO_4$ film on FTO substrate. (c) Sectioned volume with a cylindrical $\Phi 15 \times 60$ nm$^3$ region across the $BiVO_4$/FTO interface, visually separated by the iso-composition surface of 12.5 at.% Bi, and (d) composition within the cylinder from top to bottom.

## Calculation of Stability Number

According to Ref.[25], the stability number $S$ describes the ratio between the number of evolved $O_2$ molecules and the number of dissolved ions. It can be evaluated either by integrated or instantaneous quantities as follows:

$$S = \frac{Q}{zFn} = \frac{i}{zF\dot{n}}$$

, where $Q$ and $i$ are the total charge and current density, respectively; $z = 4$ is the number of electron (hole) transfer to evolve one $O_2$ molecule during OER; $F = 96485$ C mol$^{-1}$ is the Faraday constant; $n$ and $\dot{n}$ are the total number of dissolved ions and the instantaneous dissolution rates, respectively.